Journal of Petroleum Science and Engineering 76 (2011) 116–123

Contents lists available at ScienceDirect

Journal of Petroleum Science and Engineering

journal homepage: www.elsevier.com/locate/petrol

On the feasibility of inducing oil mobilization in existing reservoirs via wellbore harmonic fluid action

Chanseok Jeong [a], Chun Huh [b], Loukas F. Kallivokas [a,*]

[a] Department of Civil, Architectural and Environmental Engineering, The University of Texas at Austin, 1 University Station, C1748, Austin, TX 78712, USA
[b] Department of Petroleum and Geosystems Engineering, The University of Texas at Austin, 1 University Station, C0300, Austin, TX 78712, USA

ARTICLE INFO

Article history:
Received 11 September 2009
Accepted 10 January 2011
Available online 23 January 2011

Keywords:
Wave-based EOR
Vibrational energy delivery
Fractured reservoir
Oil mobilization

ABSTRACT

Although vibration-based mobilization of oil remaining in mature reservoirs is a promising low-cost method of enhanced oil recovery (EOR), research on its applicability at the reservoir scale is still at an early stage. In this paper, we use simplified models to study the potential for oil mobilization in homogeneous and fractured reservoirs, when harmonically oscillating fluids are injected/produced within a well. To this end, we investigate first whether waves, induced by fluid pressure oscillations at the well site, and propagating radially and away from the source in a homogeneous reservoir, could lead to oil droplet mobilization in the reservoir pore-space. We discuss both the fluid pore-pressure wave and the matrix elastic wave cases, as potential agents for increasing oil mobility. We then discuss the more realistic case of a fractured reservoir, where we study the fluid pore-pressure wave motion, while taking into account the leakage effect on the fracture wall.

Numerical results show that, in homogeneous reservoirs, the rock-stress wave is a better energy-delivery agent than the fluid pore-pressure wave. However, neither the rock-stress wave nor the pore-pressure wave is likely to result in any significant residual oil mobilization at the reservoir scale. On the other hand, enhanced oil production from the fractured reservoir's matrix zone, induced by cross-flow vibrations, appears to be feasible. In the fractured reservoir, the fluid pore-pressure wave is only weakly attenuated through the fractures, and thus could induce fluid exchange between the rock formation and the fracture space. The vibration-induced cross-flow is likely to improve the imbibition of water into the matrix zone and the expulsion of oil from it.

1. Introduction

As is well known, no more than 10% to 20% of the original oil in place (OOIP) is produced by the primary oil recovery mechanism, whereas an additional 20% to 30% OOIP may be recovered through waterflooding, or similar methods. However, even after extensive waterflooding, a significant amount of oil is still left in the reservoir. While various enhanced oil recovery (EOR) methods can be used to displace some of the remaining oil (Lake, 1989), most such methods remain expensive and manpower-intensive. So-called, seismic-wave-based EOR methods have been suggested as a low-cost and environmentally friendly alternative to conventional EOR methods, partially supported by scant field observations. The key premise of wave-based EOR methods hinges on the ability of wave sources, whether on the surface or elsewhere (well, reservoir, etc.), to deliver sufficient vibrational energy to an existing reservoir to induce oil mobility.

* Corresponding author. Tel.: +1 512 232 5769; fax: +1 512 471 7259.
E-mail addresses: chanseok.jeong@gmail.com (C. Jeong), chunhuh@mail.utexas.edu (C. Huh), loukas@mail.utexas.edu (L.F. Kallivokas).

0920-4105/$ – see front matter © 2011 Elsevier B.V. All rights reserved.
doi:10.1016/j.petrol.2011.01.005

A number of field observations seem to support the basic hypothesis that there is a connection between increased oil production rates and reservoir shaking, even though the precise mechanisms are not well understood (see, however, Beresnev (2006), for the theory and quantification of a candidate mechanism). For example, increased oil production rates have been reported in the aftermath of earthquakes (Steinbrugge and Moran, 1954; Smimova, 1968; Voytov et al., 1972; Osika, 1981); the increased rates were sustained for a few days post the main seismic event, without necessarily the presence/aid of strong aftershocks. Field applications of wave-based EOR in existing oil fields, where the vibrations were induced by either ground-surface or borehole wave sources, have also reportedly resulted in increased oil production rates (Kuznetsov and Nikolaev, 1990; Kouznetsov et al., 1998; Westermark et al., 2001; Kuznetsov and Simkin, 2002; Guo et al., 2004; Zhu and Xutao, 2005).

Despite field evidence, to date, the underlying physics are still not well understood, and the literature is rather thin on the matter: exceptions include the work by Beresnev and Johnson (1994), who suggested the loss or reduction of oil droplet adherence to the pore-surface wall, due to the wall's oscillation, as the predominant mechanism for wave-based EOR. To investigate the effect the waves have on the motion of an oil droplet entrapped in the pore-space, Iassonov and Beresnev (2003) built a threshold capillary-trapping model of an oil droplet in a porous medium, and subjected it to low-frequency vibration. Subsequent experimental investigations (Li et al., 2005), and numerical simulations (Beresnev, 2006), indicated that a sufficiently large acceleration of the pore-surface wall must be induced, at least of the order of 1 to 10 m/sec^2, in order to mobilize the oil droplet in the pore-space by the vibrating pore-surface walls. However, Beresnev also indicated that very low accelerations may be sufficient for mobilizing significant oil volumes, depending on the ganglion colony's mobility threshold.

An alternative interpretation was offered by Surguchev et al. (2002), and Huh (2006) who suggested that the waves can increase the mobility of the reservoir's remaining oil due to their ability to induce cross-flow in a heterogeneous reservoir. In such a reservoir, it is quite difficult to deliver injection fluids to the low permeability areas where, typically, the oil is bypassed. However, the waves illuminate indiscriminately both the low- and high-permeability reservoir regions, and can thus induce differential pore-pressure between layers of different permeability. Since the amplitude of the pore-pressure oscillation is larger in a low-permeability area than in a high-permeability area (Bachrach et al., 2001), the pressure gradient between the two areas could lead to cross-flow, which effectively mobilizes the residual oil from the low- to the high-permeability area.

It is thus of interest to examine whether wave sources could stimulate sufficiently a formation to overcome the mobility threshold of residual oil; of particular interest is whether waves traveling through the matrix or through the fluid (the pore-pressure waves) are better energy-delivery agents. In this paper, we study numerically the potential for oil mobility stimulation at the reservoir-scale due to vibrations induced by means of a wellbore hydraulic pressure wave source (Fig. 1), using simplified models, in an attempt to quantify the potential for increasing oil mobility; the case of sources located on the ground surface, though more promising, is not discussed herein. We report first on the wave motion solution in a homogeneous oil reservoir; we study two cases, depending on whether the fluid or the matrix is excited (but we do not consider the coupled poroelastic case). To assess the feasibility of oil mobilization at the pore-space, we use a recently developed correlation between the oil mobilization index and the wave-induced displacement field (Huh, 2006).

In the second part of the paper, we investigate whether vibrational energy could induce cross-flow in a fractured reservoir. Water pressure pulsations are considered to be an effective way to accelerate oil mobilization, since cross-leakage flow could occur between the fracture reservoir part and the rock formation (Surguchev et al., 2002). We examine whether there could arise a sufficient rate of cross-leakage flow to displace oil from the rock formation into the fractures of the reservoir.

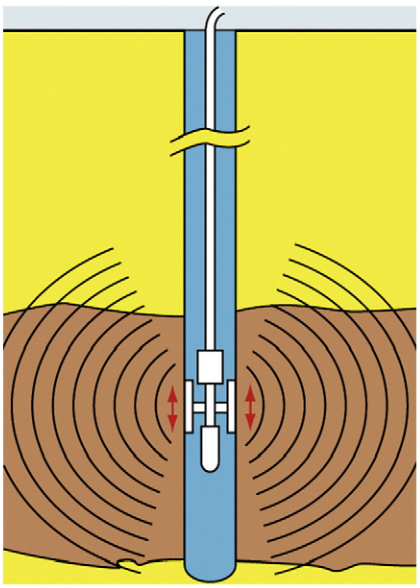

Fig. 1. Schematic of wellbore wave source.

2. Wave motion in homogeneous oil reservoirs

To assess the feasibility of mobilizing typically bypassed oil by vibrational means, we examine the closed-form solutions of the time-harmonic wave motion in a homogeneous reservoir induced by a wellbore-pressure wave source. For simplicity, we treat the axisymmetric problem, whereby the source is assumed to act on the walls of a well of infinite depth (Fig. 2).

We obtain solutions for two limiting cases: (1) the pore-pressure wave arising when the fluid alone is excited; and (2) the stress wave of the reservoir rock arising when the matrix alone is excited. By comparing the wave behavior of these two limiting cases, we try to assess the effectiveness of delivering vibrational energy at a distance from the wellbore source.

2.1. Radial propagation of fluid pressure wave in a homogeneous reservoir

To estimate how the pressure waves propagate into the reservoir, we adopt the transient pressure diffusion equation that is commonly employed to interpret pressure test results (Matthews and Russell, 1967). Implicit in this approach is the assumption that the pressure oscillation generated at the well wall propagates only through the pore space, while the reservoir rock remains dormant. Assuming further that the pore-pressure wave propagates only in the radial direction, the pressure distribution can be calculated from (Matthews and Russell, 1967):

$$\frac{1}{r}\frac{\partial}{\partial r}\left(r\frac{\partial p(r,t)}{\partial r}\right) = \frac{\phi\eta c_t}{k_r}\frac{\partial p(r,t)}{\partial t}, \tag{1}$$

where $p(r,t)$ is the fluid pressure; r denotes radial coordinate; t is time; η is viscosity; k_r is permeability; ϕ is porosity; and $c_t = c_w + c_r$ denotes compressibility, with c_w being the fluid, and c_r the rock compressibility, respectively. The boundary condition at the well wall $(r = r_w)$ is:

$$p(r_w, t) = \hat{p}_w e^{i\omega t}, \tag{2}$$

where $\hat{p}_w$ is the input pressure amplitude (this pressure is in addition to the static reservoir pressure). At the far field, there also holds:

$$\lim_{r\to\infty} p(r,t) = 0. \tag{3}$$

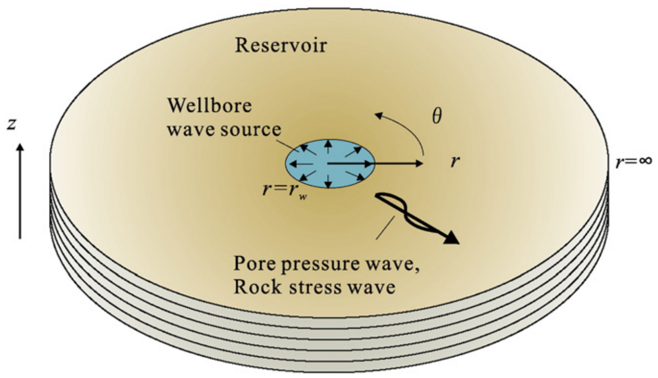

Fig. 2. Wave propagation in a permeable elastic medium induced by a wellbore hydraulic pump wave source.

Since the resulting pressure wave will also be harmonic, i.e., $p(r,t) = \hat{p}(r)e^{i\omega t}$, Eq. (1) reduces to:

$$\frac{\partial^2 \hat{p}}{\partial r^2} + \frac{1}{r}\frac{\partial \hat{p}}{\partial r} - \beta^2 \hat{p} = 0, \quad \text{with} \quad \beta^2 = \frac{i\omega\phi\eta c_t}{k_r}. \tag{4}$$

The general solution to the above equation is:

$$\hat{p}(r) = a_1 I_0(\beta r) + a_2 K_0(\beta r), \tag{5}$$

where I_0 and K_0 are the zeroth-order modified Bessel functions of the first and second kind, respectively. To satisfy the radiation condition, Eq. (3), a_1 should vanish. Then, using the boundary condition, Eq. (2), there results:

$$\hat{p}(r) = \hat{p}_w \frac{K_0(\beta r)}{K_0(\beta r_w)}. \tag{6}$$

2.2. Pore-pressure wave amplitude decay in a homogeneous reservoir

Because the pressure propagation in the reservoir is of a diffusive nature, the pressure oscillation amplitude decreases with distance from the wellbore, largely depending on the pressure diffusivity parameter $\beta^2 = i\omega\phi\eta c_t / k_r$. Fig. 3 shows the effects of the oscillation frequency (ω) on the pressure amplitude (normalized with respect to the source amplitude $\hat{p}_w$), as a function of the radial distance r from the wellbore (the curves are shown on a semilog scale; the ordinate represents the modulus of the pressure amplitude $\hat{p}(r)$, which is, in general, complex). For the curves shown, we used $\eta = 1$ cp ($= 0.001$ Pa sec), $k_r = 100$ md ($= 9.87 \times 10^{-14}$ m^2), $\phi = 0.3$, $r_w = 0.06$ m, and $c_t = 1.5 \times 10^{-9}$ Pa^{-1}.

We observe that the pressure amplitude decreases very rapidly with distance, unless the frequency is extremely low (0.1 Hz). This is expected since, due to the tortuosity of the pore space, the pressure wave attenuates fairly fast. In general, the pressure wave propagation is governed by the diffusivity parameter: as the fluid viscosity or the compressibility increases, or the permeability decreases, the diffusivity β increases, and the pressure amplitude attenuates more sharply. We discuss next the elastic (rock) wave.

2.3. Radial propagation of rock wave in a homogeneous reservoir

Whereas, owing to the tortuosity of the pore space, the propagation of fluid pressure oscillations through the pore space is highly attenuated, the propagation of elastic deformation in the

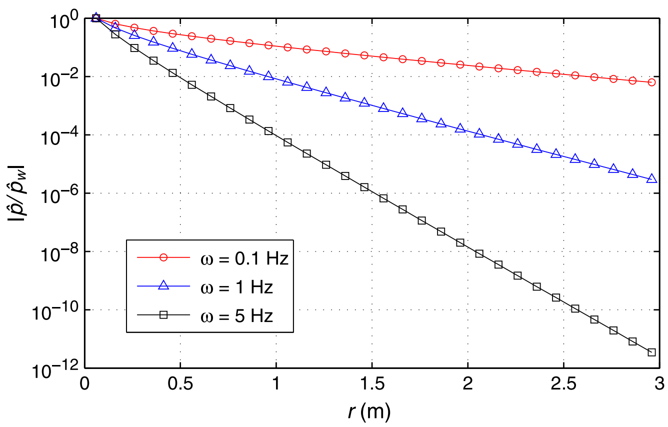

Fig. 3. Modulus of normalized pressure wave $p_r / \hat{p}_w$ in a homogeneous reservoir–pore pressure solution only as a function of distance from the wellbore source; various excitation frequencies.

reservoir rock could be more effective. When a pressure oscillation is applied at the well wall by injecting (or producing) a fluid, the rock face at the wellbore will be deformed, and the deformation will propagate through the reservoir's matrix, engaging both the matrix and the fluid. In the interest of an approximate assessment, we will assume that the reservoir is a homogeneous elastic medium, and will not consider the coupled poroelastic case. While highly simplistic, the model allows for the study of the vibrational energy propagation through the reservoir rock. For the axisymmetric problem considered herein, the following equation of motion holds:

$$\frac{\partial \sigma_{rr}}{\partial r} + \frac{\sigma_{rr} - \sigma_{\theta\theta}}{r} = \rho \frac{\partial^2 u_r}{\partial t^2}. \tag{7}$$

where (r,θ) denote polar coordinates; t is time; ρ is the composite density of the matrix and the fluid; u_r denotes radial displacement; and σ denotes the stress tensor. We assume further the presence of material damping, which we express in terms of a Voigt model (White, 1983). Then, the constitutive law becomes:

$$\sigma_{ij} = \lambda\varepsilon_{kk}\delta_{ij} + 2\mu\varepsilon_{ij} + \lambda' \frac{\partial \varepsilon_{kk}}{\partial t}\delta_{ij} + 2\mu' \frac{\partial \varepsilon_{ij}}{\partial t}, \quad (i,j = r,\theta) \tag{8}$$

where λ, and μ are the Lamé constants with $\lambda = 2\mu\nu/(1-2\nu)$, and ν denoting Poisson's ratio; δ_{ij} is the Kronecker delta; λ' and ν' are viscous loss parameters; ε is the strain tensor, and repeated indices imply summation. Due to the assumption of axisymmetry, the only surviving strain tensor components are:

$$\varepsilon_{rr} = \frac{\partial u_r}{\partial r}, \quad \varepsilon_{\theta\theta} = \frac{u_r}{r}. \tag{9}$$

Substitution of Eqs. (8) and (9) into the equation of motion, Eq. (7), results in:

$$\left\{\frac{\partial^2 u_r}{\partial r^2} + \frac{1}{r}\frac{\partial u_r}{\partial r} - \frac{u_r}{r^2}\right\} + \alpha \frac{\partial}{\partial t}\left\{\frac{\partial^2 u_r}{\partial r^2} + \frac{1}{r}\frac{\partial u_r}{\partial r} - \frac{u_r}{r^2}\right\} = \frac{1}{c^2}\frac{\partial^2 u_r}{\partial t^2}, \tag{10}$$

where c denotes the dilatational wave velocity $c = \sqrt{(\lambda + 2\mu)/\rho}$, and $\alpha = (\lambda' + 2\mu')/(\lambda + 2\mu)$ is the attenuation factor. Assuming a harmonic solution of the form $u_r(r,t) = \hat{u}_r(r)e^{i\omega t}$, Eq. (10) reduces to:

$$\frac{\partial^2 \hat{u}_r}{\partial r^2} + \frac{1}{r}\frac{\partial \hat{u}_r}{\partial r} - \frac{\hat{u}_r}{r^2} + k^2 \hat{u}_r = 0, \tag{11}$$

where $k = \frac{\omega}{c}\sqrt{\frac{1 - i\omega\alpha}{1 + (\omega\alpha)^2}}$. With the introduction of the auxiliary variable $z = kr$, Eq. (11) becomes:

$$z^2 \frac{\partial^2 \hat{u}_r}{\partial z^2} + z\frac{\partial \hat{u}_r}{\partial z} + \left(z^2 - 1\right)\hat{u}_r = 0. \tag{12}$$

The general solution of Eq. (12) is

$$\hat{u}_r(z) = c_1 H_1^{(1)}(z) + c_2 H_1^{(2)}(z), \tag{13}$$

where $H_1^{(1)}(z)$ and $H_1^{(2)}(z)$ are the first-order Hankel functions of the first and second kind, respectively. To obtain the constants in Eq. (13), we first look at the asymptotic behavior of Hankel functions, $H_1^{(1)}(z)$ and $H_1^{(2)}(z)$ (Abramowitz and Stegun, 1964) :

$$H_1^{(1)}(z) = H_1^{(1)}(kr) \sim \sqrt{\frac{2}{\pi kr}} e^{i\left(kr - \frac{3\pi}{4}\right)}, \tag{14}$$

$$H_1^{(2)}(z) = H_1^{(2)}(kr) \sim \sqrt{\frac{2}{\pi kr}} e^{-i\left(kr - \frac{3\pi}{4}\right)}. \tag{15}$$

When the time-dependent term ($e^{i\omega t}$) is taken into account, Eqs. (14) and (15) represent incoming and outgoing propagating waves, respectively. Since the generated waves ought to be outgoing, c_1 in Eq. (13) vanishes, and the general solution for the amplitude of the radial displacement reduces to:

$$\hat{u}_r(r) = c_2 H_1^{(2)}(kr). \tag{16}$$

To resolve the last remaining constant c_2, we use the boundary condition at the well wall

$$\sigma_{rr}(r_w, t) = -\hat{p}_w e^{i\omega t}. \tag{17}$$

In the frequency domain, the radial stress component can be cast as

$$\hat{\sigma}_{rr} = (\lambda + 2\mu)(1 + \alpha i\omega)\hat{\varepsilon}_{rr}, \tag{18}$$

where we assumed that $\sigma_{rr} = \hat{\sigma}_{rr} e^{i\omega t}$, $\varepsilon_{rr} = \hat{\varepsilon}_{rr} e^{i\omega t}$. Then,

$$\hat{\varepsilon}_{rr} = \frac{\partial \hat{u}_r(r)}{\partial r} = \frac{\partial}{\partial r}\left[c_2 H_1^{(2)}(kr)\right] = c_2 k\left[H_0^{(2)}(kr) - \frac{1}{kr} H_1^{(2)}(kr)\right]. \tag{19}$$

Inserting Eq. (19) into Eq. (18), while taking into account the boundary condition Eq. (17), yields the constant c_2 as:

$$c_2 = -\frac{\hat{p}_w}{(\lambda + 2\mu)(1 + \alpha i\omega)k\left[H_0^{(2)}(kr_w) - \frac{1}{kr_w} H_1^{(2)}(kr_w)\right]}. \tag{20}$$

Thus, the solution for the amplitude of the rock displacement in the frequency-domain becomes:

$$\hat{u}_r(r) = -\frac{\hat{p}_w H_1^{(2)}(kr)}{(\lambda + 2\mu)(1 + \alpha i\omega)k\left[H_0^{(2)}(kr_w) - \frac{1}{kr_w} H_1^{(2)}(kr_w)\right]}. \tag{21}$$

2.4. Rock wave amplitude decay in a homogeneous reservoir

Figs. 4 and 5 show the radial deformation amplitude of the matrix rock $\hat{u}_r(r)$, when there is damping ($\alpha = 0.03$ sec), as a function of distance. We used a wellbore pressure oscillation amplitude $p_w = 2 \times 10^6$ Pa, a wave source frequency $\omega = 1$ Hz, shear modulus $\mu = 6 \times 10^8$ Pa, Poison's ratio $\nu = 0.3$, mass density $\rho = 2100$ kg/m^3, and wave velocity $c = 1000$ m/s. Fig. 4 shows the real and imaginary parts of $\hat{u}_r(r)$. As the rock deformation propagates, some phase shift also occurs, and with $\omega = 1$ Hz, the wavelengths are fairly large, and the resulting motion is quite small. Fig. 5 depicts the modulus of $\hat{u}_r(r)$ plotted in semi-log scale as a function of distance and for several excitation frequencies; all curves clearly exhibit the expected exponential decay. However, a comparison of the pressure wave decay performance shown earlier in Fig. 3 for the purely diffusive propagation of the pore fluid, and those of Figs. 4 and 5 for the rock wave case, shows much more rapid decay associated with the former case than the latter. In short, it appears that the elastic wave is a more effective vibrational energy delivery agent than the pore-pressure waves, as also mentioned in Pride et al. (2008).

Fig. 6 shows the dependence of the amplitude of the stress wave on the attenuation factor. As expected, the rock deformation wave attenuates faster as the attenuation factor increases.

2.5. Oil mobility estimation in a homogeneous reservoir

To obtain a qualitative estimate on the effectiveness of the mobilization of oil remaining in a homogeneous reservoir, we adopt the approach proposed earlier by Huh (2006). Figs. 7 and 8 (originally depicted in Huh (2006)) show residual oil displacement efficiency curves in terms of the rock displacement amplitude and the excitation frequency for two different pore radii of 100 μm and 200 μm, respectively. The underlying approximate model is based on the calculation of the average fluid velocity in a pore in response to rock oscillation, and then estimation of the residual oil mobilization efficiency by using the well-known Capillary Number Correlation (Pope and Baviere, 1991). In Figs. 7 and 8, S_o denotes the post-vibration residual oil, whereas S_{ori} denotes the residual oil originally

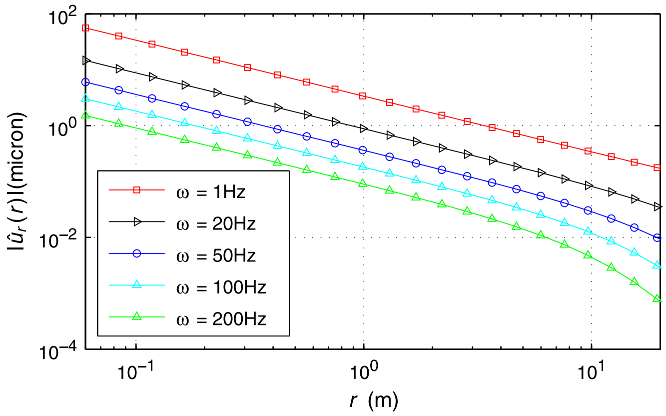

Fig. 5. Modulus of the displacement field of the rock stress wave $\hat{u}_r(r)$ as a function of distance for several frequencies (wave velocity $c = 1000$ m/s, attenuation factor $\alpha = 0.03$ sec).

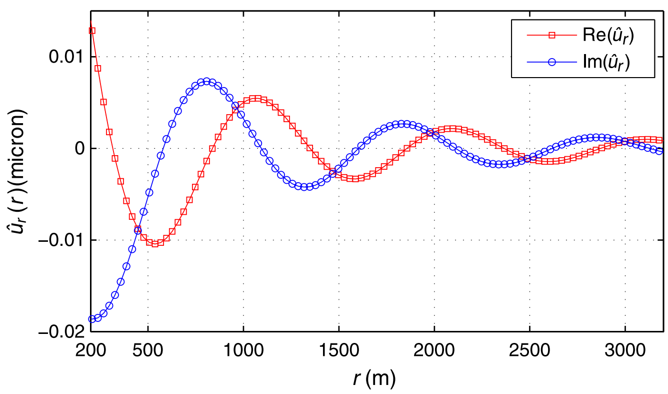

Fig. 4. Real and imaginary parts of the wave amplitude displacement field $\hat{u}_r(r)$ as a function of distance (rock velocity $c = 1000$ m/s, attenuation factor $\alpha = 0.03$ sec, source frequency $\omega = 1$ Hz).

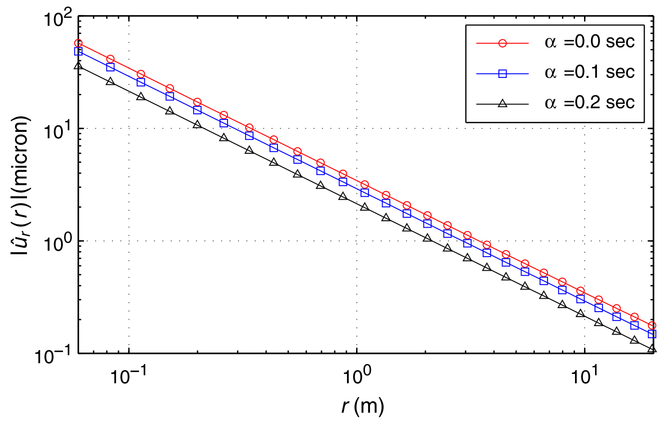

Fig. 6. Modulus of the displacement field of the rock stress wave $\hat{u}_r(r)$ as a function of distance for several attenuation factors (wave velocity $c = 1000$ m/s, frequency $\omega = 1$ Hz).

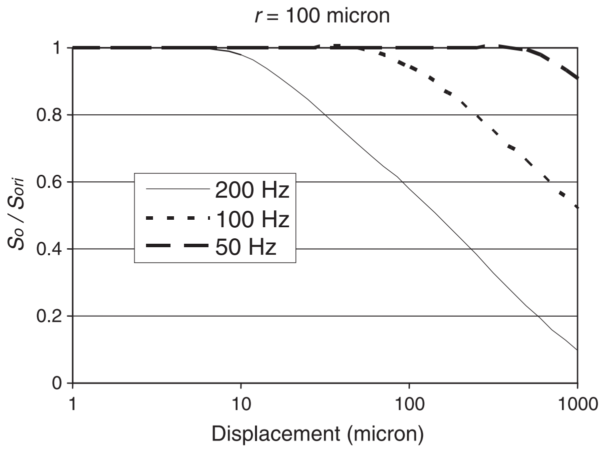

Fig. 7. Residual oil displacement efficiency with respect to the rock displacement and the frequency for a pore radius of 100 μm.

contained in the rock formation. Therefore, $S_o/S_{ori}=1$ implies that no oil is mobilized, while $S_o/S_{ori}=0$ means that all residual oil is mobilized. Figs. 7 and 8 suggest that oil mobilizes more easily: (1) when the rock displacement is larger; (2) when the excitation frequency is higher, and; (3) when the pore is wider.

We use the previously obtained rock displacement amplitudes due to the wellbore source as input to the Huh model (for various excitation frequencies), in order to estimate the oil mobilization index S_o/S_{ori}. To this end, Table 1 lists the mobilization index in the neighborhood of the wellbore source, i.e., for distances ranging between 0.07 and 5 m. We assumed a pore radius of 200 μm, attenuation factor $\alpha=0.01$ sec, and amplitude of the wellbore pressure oscillation p_w of 2×10^6 Pa. As it can be seen from Table 1, some oil mobilization occurs at higher frequencies, whereas there is, effectively, no oil mobilization for lower frequencies. For a pore radius of 100 μm, which represents lower-permeability rock, the residual oil mobilization efficiency decreases even further.

3. Wave motion in the fractured reservoir

3.1. Propagation of fluid pressure wave in the fractured space

As discussed in Section 2.1, the fluid pore-pressure wave attenuates fairly rapidly with distance because its propagation through the tortuous pore pathways is highly impeded. On the other hand, if the reservoir has a network of fractures which have

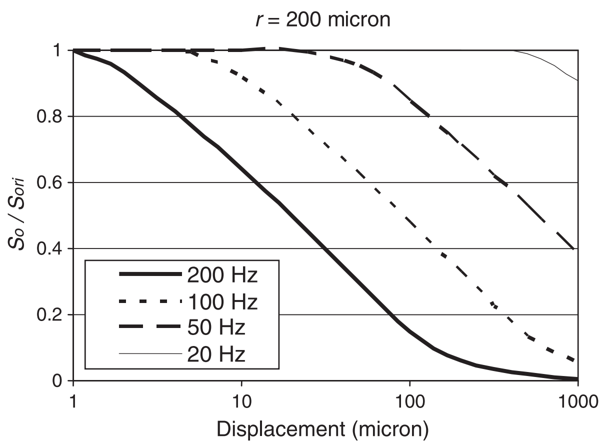

Fig. 8. Residual oil displacement efficiency with respect to the rock displacement and the frequency for a pore radius of 200 μm.

Table 1
Mobilization index S_o/S_{ori} at locations proximal to the source; various frequencies.

r(m)	$\omega=200$Hz		$\omega=100$Hz		$\omega=50$Hz		$\omega=20$Hz	
	$\lvert\hat{u}_r\rvert$(μm)	$\frac{S_o}{S_{ori}}$	$\lvert\hat{u}_r\rvert$(μm)	$\frac{S_o}{S_{ori}}$	$\lvert\hat{u}_r\rvert$(μm)	$\frac{S_o}{S_{ori}}$	$\lvert\hat{u}_r\rvert$(μm)	$\frac{S_o}{S_{ori}}$
0.07	3.88	0.82	7.70	0.95	14.9	0.99	30.5	1
0.1	2.72	0.89	5.39	0.97	10.4	1	21.4	1
1	0.263	1	0.531	1	1.04	1	2.14	1
5	0.0313	1	0.0808	1	0.186	1	0.435	1

medium to high permeability, the pressure wave could propagate rapidly through that network, with amplitude that still maintains a reasonable magnitude away from the wellbore. The pressure oscillation in a fracture could bring about an exchange of fluids between the fractures and the matrix, thereby potentially enhancing the imbibition of injected water (or surfactant) into the matrix, and the subsequent expulsion of oil from the matrix.

In this section, we estimate the pressure distribution in the fracture when fluid oscillations are initiated at the wellbore, and study whether the propagation of pressure waves through a fracture network can effectively induce exchange of fluids between the fracture and the matrix. For simplicity, the propagation of pressure wave is considered in a 1D fracture (Fig. 9). We assume that the vertical fracture has a uniform gap width w, length x_f, height h, and constant permeability k_f. We denote by q_f the rate of fluid leakage from the fracture into the matrix zone.

At the wellbore ($x=0$), a periodic injection/production of fluid is applied with a frequency of ω:

$$q_w(t) = \hat{q}_w e^{i\omega t}, \tag{22}$$

where $\hat{q}_w$ is the rate amplitude (q_w, and $\hat{q}_w$ are fluid volume rates). The pressure distribution in the fracture can be calculated from the pressure transient equation (Cinco-L. et al., 1978):

$$\frac{\partial^2 p_f(x,t)}{\partial x^2} - \frac{\eta}{k_f}\frac{q_f(x,t)}{wh} = \frac{\phi_f \eta c_{tf}}{k_f}\frac{\partial p_f(x,t)}{\partial t}, \tag{23}$$

where $p_f(x,t)$ is the fluid pressure distribution; η is the viscosity; k_f is permeability; ϕ_f is porosity; $c_{tf}=c_w+c_f$, where c_w is fluid compressibility, and c_f is fracture compressibility; and $q_f(x,t)$ is the fluid leakage rate (measured in volume rate per unit length) into the rock formation. The boundary conditions are:

$$\frac{\partial p_f}{\partial x} = -\frac{\eta q_w}{2whk_f}, \quad \text{at} \quad x=0, \tag{24}$$

$$\frac{\partial p_f}{\partial x} = 0, \quad at \quad x = x_f. \tag{25}$$

The pressure distribution in the formation can be obtained from the pressure transient equation:

$$\left(\frac{\partial^2}{\partial x^2} + \frac{\partial^2}{\partial y^2}\right) p_r(x,y,t) = \frac{\phi_r \eta c_{tr}}{k_r}\frac{\partial p_r(x,y,t)}{\partial t}, \tag{26}$$

where $p_r(x,y,t)$ denotes the pressure in the formation, ϕ_r, k_r, and c_{tr} are porosity, permeability, and total compressibility, respectively, for the rock formation. The interface conditions are:

$$p_r = p_f, \quad \text{at} \quad y=0 \quad \text{and} \quad 0\le x\le x_f, \tag{27}$$

$$\frac{\partial p_r}{\partial y} = -\frac{nq_f}{2hk_r} \quad at \quad y=0 \quad and \quad 0\le x\le x_f, \tag{28}$$

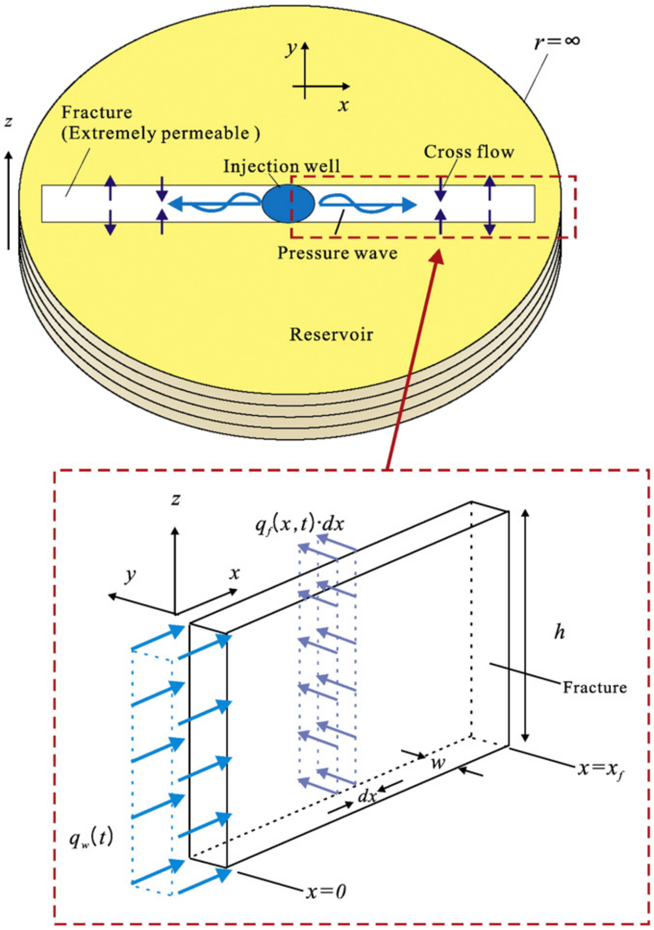

Fig. 9. Propagation of pressure wave in a fractured reservoir. Fluid is injected into the fracture at a rate of $q_w(t)$, with fluid leaking through the fracture wall at a rate $q_f(x,t)$.

and the radiation condition is:

$$\lim_{x,y\to\infty} p_r = 0. \tag{29}$$

We assume time-harmonic solution of the form:

$$\begin{aligned} p_f(x,t) &= \hat{p}_f(x)e^{i\omega t}, \\ q_f(x,t) &= \hat{q}_f(x)e^{i\omega t}, \\ p_r(x,t) &= \hat{p}_r(x)e^{i\omega t}. \end{aligned} \tag{30}$$

We discuss two cases: first, if the leakage effect is assumed to be negligible, Eq. (23) reduces to the pressure diffusion equation in the fracture:

$$\frac{\partial^2 \hat{p}_f(x)}{\partial x^2} - D_f^2 \hat{p}_f(x) = 0, \quad D_f^2 = \frac{i\omega\phi_f \eta c_{tf}}{k_f}. \tag{31}$$

The solution of Eq. (31) is:

$$\hat{p}_f(x) = a_1 e^{D_f x} + a_2 e^{-D_f x}. \tag{32}$$

Using the boundary conditions Eqs. (24) and (25), we obtain for the amplitude of the pressure in the fracture:

$$\hat{p}_f(x) = \frac{R_f}{D_f} \frac{\cosh\left[D_f\left(x_f - x\right)\right]}{\sinh\left[D_f x_f\right]}, \tag{33}$$

where

$$R_f = \frac{\eta \hat{q}_w}{2whk_f}. \tag{34}$$

On the other hand, if there is a significant leakage of fluids from the fracture to the formation, Eqs. (23) and (26) need to be solved simultaneously. Accordingly, we seek solutions of the form:

$$p_r(x,y,t) = \hat{p}_{rx}(x)e^{-D_r y}e^{i\omega t}, \quad D_r^2 = \frac{i\omega\phi_r \eta c_{tr}}{k_r} \tag{35}$$

which satisfies Eq. (26) provided that:

$$\frac{\partial^2 \hat{p}_{rx}(x)}{\partial x^2} = 0, \tag{36}$$

within the rock formation. By virtue of the interface conditions Eqs. (27) and (28):

$$\hat{p}_{rx}(x) = \hat{p}_f(x) = \frac{\eta \hat{q}_f}{2D_r hk_r}. \tag{37}$$

Using Eq. (37), Eq. (23) yields

$$\frac{\partial^2 \hat{p}_f(x)}{\partial x^2} - \left(\overline{D}_f^2\right)\hat{p}_f(x) = 0, \tag{38}$$

where

$$\overline{D}_f^2 = \frac{2k_r D_r}{k_f w} + \frac{\phi_f \eta c_{tf} i\omega}{k_f} = \frac{2k_r D_r}{k_f w} + D_f^2. \tag{39}$$

The solution of Eq. (38), valid when the leakage effect is not negligible, is obtained as:

$$\hat{p}_f(x) = \frac{R_f}{\overline{D}_f} \frac{\cosh\left[\overline{D}_f\left(x_f - x\right)\right]}{\sinh\left[\overline{D}_f x_f\right]}. \tag{40}$$

Combining either Eq. (33) or Eq. (40) with Eq. (35), the resulting amplitude of the pressure distribution within the rock formation becomes:

$$\hat{p}_r(x,y) = \hat{p}_f(x)e^{-D_r y}. \tag{41}$$

3.2. Pressure wave decay in a fractured reservoir

Figs. 10 and 11 show the effects of the oscillation frequency ω, (1) on the pressure modulus, and (2) on the leakage rate, both of which are given as a function of distance from the wellbore. In Fig. 10, the distribution of the pressure modulus is shown for the two cases that depend on whether the leakage effect is ignored or not. The pressure modulus is also shown for different frequencies ranging from 0.1 to 10 Hz in Fig. 12 (where the leakage effect is taken into account). For all plots we used $\eta = 1$ cp ($= 0.001$ Pa sec), $k_f = 5\times10^5$ md ($= 4.935\times10^{-10}$ m^2), $k_r = 100$ md ($= 9.870\times10^{-14}$ m^2), $\hat{q}_w = 10$ Barrel/day ($= 1.84\times10^{-5}$ m^3/sec), $\phi_f = 0.4$, $\phi_r = 0.2$, and $w = 0.01$ m, $h = 0.3$ m, $x_f = 20$ m, $c_{tr} = 1.5\times10^{-10}$ Pa^{-1}, and $c_{tf} = 1.5\times10^{-9}$ Pa^{-1}.

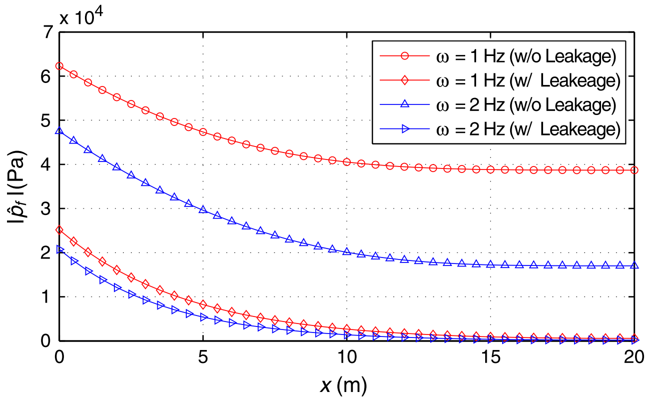

Fig. 10. Pressure oscillation amplitude versus distance in fracture for two frequencies $\omega = 1$ Hz and $\omega = 2$ Hz (shown are two cases depending on whether the wall leakage effect is ignored or not).

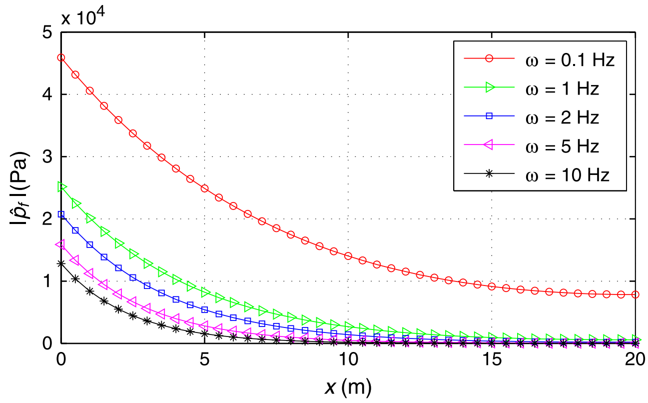

Fig. 12. Pressure oscillation amplitude versus distance in fracture for wave frequencies $\omega = 0.1$ Hz to $\omega = 10$ Hz with leakage flow on the fracture wall surface.

Comparing the pressure amplitude distributions of Figs. 10 and 12 with those for the radial cases of Fig. 3, we see that the pressure wave can propagate in the fracture much more effectively, even though the amplitude decreases with distance. As with the radial pressure diffusion cases of Fig. 3, and the elastic (rock deformation) cases of Figs. 4–6, the pressure wave propagation efficiency decreases with increase in oscillation frequency. We remark that, with leakage into the matrix zone, the modulus of pressure wave in the fracture decreases even further.

Fig. 11 shows that the amplitude of the flow rate in and out of the formation neighboring a fracture could be sizeable enough to force the oil out from the rock formation, suggesting that the vibration application to fractured reservoirs could indeed enhance oil recovery from tight matrix zones.

4. Conclusions

In this article, we use simple prototype problems to study the feasibility of vibration-based EOR for homogeneous or fractured reservoirs via wellbore oscillating fluids. To this end, this work investigated the analytical solution of time-harmonic wave motion in homogeneous and fractured reservoirs induced by fluid pressure oscillation imposed at the wellbore. In the homogeneous reservoir case, the rock stress wave delivers the wave energy more effectively than the pore-pressure wave. However, it is still difficult to generate sufficiently large displacements to stimulate oil mobilization in the pore-space of a homogeneous reservoir, using a wellbore source. We remark though that surface excitations, and focusing the wave energy to the target reservoir zone, could prove to be more effective in delivering displacement or acceleration fields capable of dislodging oil droplets than the excitation from the wellbore sources. On the other hand, it appears that generating pressure waves in a fractured reservoir can induce cross-flow, which can then displace oil from the rock matrix. The rate of cross-flow appears to be large enough to increase the rate of oil recovery from the rock formation.

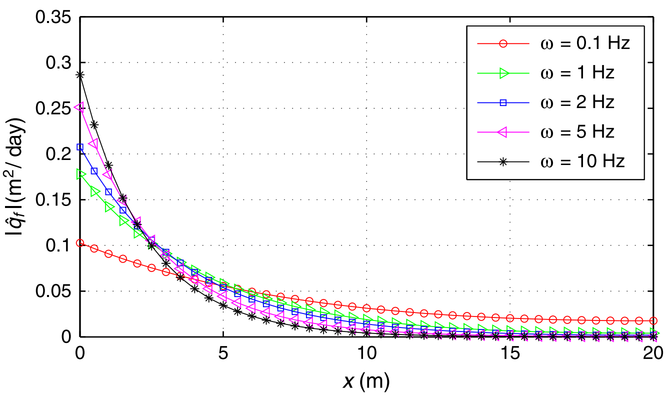

Fig. 11. Leakage rate amplitude versus distance in fracture for wave frequencies $\omega = 0.1$ Hz to $\omega = 10$ Hz.

Acknowledgments

The authors thank David Eslinger of Schlumberger, who carefully reviewed the manuscript and made many constructive suggestions. This work was partially supported by an Academic Excellence Alliance grant with KAUST, the King Abdullah University of Science and Technology. This support is gratefully acknowledged.

References

Abramowitz, M., Stegun, I., 1964. Handbook of Mathematical Functions. Dover Publication.
Bachrach, R., Nur, A., Agnon, A., 2001. Liquefaction and dynamic poroelasticity in soft sediments. J. Geophys. Res. 106, 13,515–13,526.
Beresnev, I.A., 2006. Theory of vibratory mobilization on nonwetting fluids entrapped in pore constrictions. Geophysics 71, 47–56.
Beresnev, I.A., Johnson, P., 1994. Elastic-wave stimulation of oil production: a review of methods and results. Geophysics 59, 1000–1017.
Cinco-L., H., Samaniego-V., F., Dominguez-A., N., 1978. Transient pressure behavior for a well with a finite-conductivity vertical fracture. SPE J. 253–264.
Guo, X., Du, Z., Li, G., Shu, Z., 2004. High frequency vibration recovery enhancement technology in the heavy oil fields of China. Proceedings of the SPE International Thermal Operations and Heavy Oil Symposium and Western Regional Meeting, Bakersfield, California. 16–18 March. SPE 86956.
Huh, C., 2006. Improved oil recovery by seismic vibration: a preliminary assessment of possible mechanisms. Proceedings of the International Petroleum Conference, Cancun, Mexico, Aug. 31-Sept. 2. SPE 103870.
Iassonov, P.P., Beresnev, I.A., 2003. A model for enhanced fluid percolation in porous media by application of low-frequency elastic waves. J. Geophys. Res. 108 (B3), 2138–2146.
Kouznetsov, O.L., Simkin, E.M., Chilingar, G.V., Katz, S.A., 1998. Improved oil recovery by application of vibro-energy to waterflooded sandstones. J. Petrol. Sci. Eng. 19, 191–200.
Kuznetsov, V.V., Nikolaev, A.V., 1990. Elaboration of physical principles of vibro-seismic action on oil reservoir (Razrabotka fizicheskikh osnov vibroseismicheskogo vozdeystviya na neftianouyou zalezh). A report, Institute of Physics of the Earth, Brno, Czech Republic (in Russian).
Kuznetsov, O.L., Simkin, E.M., 2002. Seismic techniques of enhanced oil recovery: experimental and field results. Energy Source 24 (9), 877–889.
Lake, L.W., 1989. Enhanced Oil Recovery. Prentice Hall.
Li, W., Vigil, R.D., Beresnev, I.A., Iassonov, P., Ewing, R., 2005. Vibration-induced mobilization of trapped oil ganglia in porous media: experimental validation of a capillary-physics mechanism. J. Colloid Interface Sci. 289, 193–199.
Matthews, C.S., Russell, D.G., 1967. Pressure buildup and ow tests in wells. SPE Monograph Series Vol. 1, Soc. Petrol. Eng.
Osika, D.G., 1981. Fluid Regime of Seismically Active Regions (Fluidniy rejim seismicheski-aktivnikh oblastey). Nauka Press. (in Russian).
Pope, G.A., Baviere, M., 1991. Reduction of capillary forces by surfactant. In: Baviere, M. (Ed.), Basic Concepts in Enhanced Oil Recovery Processes. Elsevier, pp. 89–122.
Pride, S.R., Flekkø, E.G., Aursjø, O., 2008. Seismic stimulation for enhanced oil recovery. Geophysics 73 (5), 23–35.

Smimova, M.N., 1968. Effect of earthquakes on the oil yield of the Gudermes field (Northeastern Caucasus), Izvestiya Academy of Sciences, USSR. Fizika Zemli Phys. Solid Earth 12, 71–76 (in Russian).

Steinbrugge, K.V., Moran, D.F., 1954. An engineering study of the Southern California earthquake of July 21, 1952, and its aftershocks. Bull. Seismol. Soc. Am. 44, 279–283.

Surguchev, L., Koundin, A., Melberg, O., Rolfsvåg, T., Menard, W.P., 2002. Cyclic water injection: improved oil recovery at zero cost. Pet. Geosci. 8, 89–95.

Voytov, G.I., Osika, D.G., Grechukhina, T.G., Plotnikov, I.A., 1972. Some geological and geochemical consequences of the Daghestan earthquake of May 14, 1970. Trans. USSR Acad. Sci. Earth Sci. Sect. 202, 576–579.

Westermark, R.V., Brett, J.F., Maloney, D.R., 2001. Using downhole vibration stimulation for enhanced oil recovery. World Oil 57–66.

White, J.E., 1983. Underground Sound Application of Seismic Waves. Elsevier, Amsterdam.

Zhu, T., Xutao, H., 2005. Downhole harmonic vibration oil-displacement system: a new IOR tool. Proceedings of SPE Western Regional Meeting, Irvine, California, Mar 30–Apr 01, 2005. SPE 94001-MS.